Suitability of SG Iron to Be Used As Nuclear Fuel Transport Cask

R.K.BEHERA[1], S.C.MISHRA[1], S.SEN[1]*
[1]Dept. of Metallurgical and Materials Engineering, NIT Rourkela, India-769008
*Corresponding author E-mail: sudipta58@gmail.com

J.S.DUBEY[2],
[2]Bhaba Atomic Research Centre (Post Irradiation Examination Division),
Mumbai, India-400085

Abstract— **Morphological aspects such as volume fraction of various phases, nodularity, and nodule count are responsible for mechanical properties of Spheroidal graphite cast iron (SG Iron)/ Ductile iron (DI). In present work, DI specimens were subjected to different heat treatment processes to correlate the mechanical properties with microconstituents, to be used for spent nuclear fuel cask fabrication. The investigation revealed higher strength for tempered martensitic specimens with a considerable amount of ductility. Increased Si & Cr content resulted increasing in ferrite volume fraction consequently leading to increased ductility and impact toughness, whereas increased pearlite volume fraction resulted in increased hardness.**

Keywords- ductile iron, nuclear fuel transport cask, heat treatment, mechanical property, microconstituents

I. INTRODUCTION

Spheroidal graphite cast iron is the most widely used member of cast iron family which came into being in the year 1943. It contains graphite in the form spheroids embedded in a ferritic or pearlitic matrix, rather than flakes, unlike other cast irons. The spheroidal graphite in a ferritic matrix provides an iron with good ductility & impact resistance by eliminating the stress concentration effect & with good tensile & yield strength equivalent to low carbon content. It has become more popular in various applications due to the combination of strength, hardness, impact resistance & a considerable amount of ductility. As the development progressed depending on the industrial requirement mechanical properties of DI was improved significantly by application of suitable heat treatment process that transformed the parent matrix into AUS ferritic, pearlitic/ferritic, tempered martensitic microstructures.

Ductile iron with fully ferritic matrix provides the highest amount of ductility & impact strength compared to any other matrix, whereas austempering treatment enhances strength & hardness along with fair amount of elasticity [1, 2]. Hardening & tempering treatment is applied to decrease the hardness & provide ductility coupled with significantly high strength, the latter being attained by tempering at temperatures ranging from 300°C to 450°C, depending on the chemical composition & the nodule count [3]. Metallographic aspects such as nodularity, nodule count (also referred as nodule density i.e., no. of graphite nodules/mm^2) & area fraction of particular phases play a significant role in understanding the behavior under different loading conditions & system responses. The presence of exploded graphite nodules & higher nodule count leads to decrease in hardness & wear resistance irrespective of the matrix microstructure [4]. Yang et.al [5] have studied the effect two different types of austempering procedure on DI & reported the higher value of hardness & strength in case of two-step austempering process. This two-step austempering process had resulted in finer ferrite & austenite as well as higher austenitic carbon in the matrix. They also reported that the two-step austempering process has led to high wear resistance in austempered ductile iron (ADI). Heat treatment of DI through quenching followed by tempering involves delicate processing but leads to the formation of mixed matrix microstructure & presence of retained austenite which eventually improves the strength & toughness of the material [6]. Post-treatment/reheating after quenching gives rise to lower & upper bainitic, tempered martensitic structure depending upon the quenching medium & soaking/tempering time. Longer soaking/tempering time reduces the thermal stress developed during quenching & sometimes the martensite volume fraction as in the case of the studies performed by Wen et.al [7], who observed a decrease in tensile strength & increase in ductility & toughness induced by a reduction in martensite volume fraction. They also suggested that to achieve a better combination of strength & toughness tempering of the specimen could opt which will eliminate the unfavorable effect of martensite volume fraction. Under overloading conditions, most of the conventional

Structural alloys fail by a phenomenon called microvoid coalescence. The microvoids nucleate at regions of localized strain discontinuity, such as that associated with second-phase particles, inclusion, grain boundaries, & dislocation pile-ups. As the stress in the material increases, the microvoids grow, coalesce, & eventually form a continuous fracture surface. This type of fracture exhibits numerous cuplike depressions that are referred to as dimples, & the fracture mode is known as dimple rupture. Fracture under conditions of uniaxial tensile load results in the formations of mostly equiaxed dimples bounded by a rim or lip [8].

Use of ductile iron for spent nuclear fuel cask purpose came into picture towards the end of 20th century when the necessity to store & transport the spent nuclear fuel (SNF) away from the reactor site was realized. The benefit of using DI is that it can be cast to near final cask dimensions that

Board of Research in Nuclear Science (Project Grant No. 2011/36/18-BRNS), India

reduce machining efforts/costs. The cask can be cast monolithically which eliminate welds in the containment boundary & serves both as the structural containment boundary & the gamma shield. It also eliminates the needs for the "sandwich" type designs that includes welds & are harder to fabricate. Finally, the cheap material & fabrication costs compare favorably with the traditional sandwich stainless steel cask cost. According to the ASTM A874 Draft Specification Material Properties [9], the desired mechanical properties & microstructural aspects of DI material to be used for nuclear fuel transport cask is presented in Table 1.

Mochizuki & Matsushita [10] conducted experiments to evaluate the structural integrity of spent nuclear fuel cask fabricated with an unalloyed ductile iron equivalent to FCD 37 in the JIS Standard. The fracture toughness value of ferritic ductile iron was found to be very low, but analytically it was confirmed that nodular cast iron containers are strong enough to withstand an impact load during drop tests if the applied stresses are less than the yield stress. Also, the critical flaw sizes associated with the yield stress were within the non-destructive inspection capabilities.

Many researchers all around the globe have worked on DI with varying alloying elements & also applying different heat treatment processes to develop better mechanical & tribological properties. But a very few literature is available on the microstructure-strength relationship of spheroidal graphite cast iron, also reports available on the particular use of ductile iron for nuclear fuel cask fabrication is meager. Hence, attempts have been undertaken to develop DI with tailor-made properties for particular use. The current study is focused on correlating the mechanical properties with morphological aspects of DI specimen by varying the processing conditions viz. cooling rate through oil quenching & air cooling after austenitization. The effect of alloying elements on promoting different microconstituents like ferrite, martensite & pearlite & effect of phase proportions on mechanical properties is also discussed.

Table 1: The desired mechanical properties & microstructural aspects of DI material to be used for nuclear fuel transport cask, according to ASTM A874 Draft Specification Material Properties.

Mechanical properties		**Microstructure**
UTS	45ksi (300MPa)	Essentially ferritic structure with no massive carbides.
YS	30ksi (200MPa)	> 90% type I & II graphite nodules.
Elongation	12%	< 275/mm^2 graphite nodule count.
Static fracture toughness	50ksi-√inch (55MPa-√m)	

II. EXPERIMENTAL PROCEDURE

2.1 *Specimen preparation & heat treatment*

To investigate the structure-property relationship, ductile iron test blocks with different alloying elements were brought from L&T Kansbahal, India. The chemical composition of two different test blocks by weight percentage is presented in Table 2. Flat sub size tensile & Izod impact test specimens following ASTM E8 & D256 standards respectively were machined from the test blocks at M/S Steelage Engineering works, a nearby engineering workshop in Rourkela, India. Specimens were then austenitized at 1000°C for 90 minutes followed by air cooling to room temperature for normalizing heat treatment. On the other hand specimens after austenitization were quenched in mineral oil maintained at 100°C & immediately after quenching, tempered at 500°C for 120 minutes followed by air cooling to room temperature for quench & tempering heat treatment process. To obtain dual matrix structure (ferritic + martensitic) specimens were austenitized partially to 800°C and hold there for 2minutes followed by quenched to room temperature in mineral oil maintained at 100°C. After heat treatment oxide layer from each of the specimen was removed by conventional filing & emery paper polishing.

2.2 *X-ray diffraction study*

X-ray diffraction test was carried out with the help of PanAlytical - PPW3040/00 X-ray diffractometer using filtered Cu K_{α}-radiation (λ = 0.1542 nm) for a range of 40°-90° at a scanning rate of 10°/min. The obtained pattern for each specimen was analyzed by Xpert Highscore & JCPDS software to determine the crystal structure & confirmation of phases present in respective specimens.

2.3 *Metallographic & Fractographic study*

The standard metallographic technique was followed for microstructural investigation & metallographic aspects were determined using Metal Power Image analyzer at 100X magnification. Specimens were first polished with belt polisher followed by 1/0, 2/0, 3/0, 4/0 grades of emery paper & finally cloth polishing was done with alumina slurry followed by diamond polishing. The quantitative metallographic analysis was carried out on each of the specimens to determine nodularity & area fraction of different microconstituents obtained in the respective heat treated & as-cast specimens according to ASTM E2567 - 13a. Table 3 & 4 summarizes the result of the quantitative metallographic analysis. To investigate the fracture phenomenon after the tensile test, specimens were observed under the JEOL - JSM6480LV Scanning Electron Microscope (SEM) at 250X.

Table 2: Chemical composition of specimens in wt. %

Element	SG - 2	SG - 9
C	3.61	3.45
Si	2.1	2.07
Mn	0.2	0.15
S	0.007	0.008
P	0.022	0.024
Cr	0.03	0.02
Ni	0.47	0.15
Mo	0.001	----
Cu	0.009	----
Mg	0.043	0.043
Ce	0.004	----
Fe	Rest	Rest

2.4 *Mechanical property determination*

INSTRON 1195 Universal Testing Machine was used to obtain the UTS, 0.2% YS, % elongation of each heat treated & as-cast specimen by applying a maximum load of 50KN at a crosshead speed of 1mm/min. VEEKAY - TL VS4 Izod impact tester was used for obtaining the Izod impact energy of respective specimens at room temperature, applying 21.7J hammer blow at a striking angle of 150°. Vickers hardness was measured by applying a load of 20Kg & dwell time being 10seconds on each heat treated & as-cast specimen. Table 5 summarizes the average value of strength, hardness, % elongation & Izod impact energy of respective specimens.

III. RESULTS & DISCUSSIONS

3.1 *X-ray diffraction analysis*

The X-ray diffraction patterns for SG-9 & SG-2 alloys are shown in Fig.1 (a) & Fig.1 (b) respectively. BCC crystallographic planes (110), (200) & (211), suggesting the presence of ferrite, pearlite and martensite as the matrix microstructure for respective as-cast & heat treated specimens were obtained in both alloys. Final confirmation of matrix microstructure for each specimen was obtained through microscopic examination.

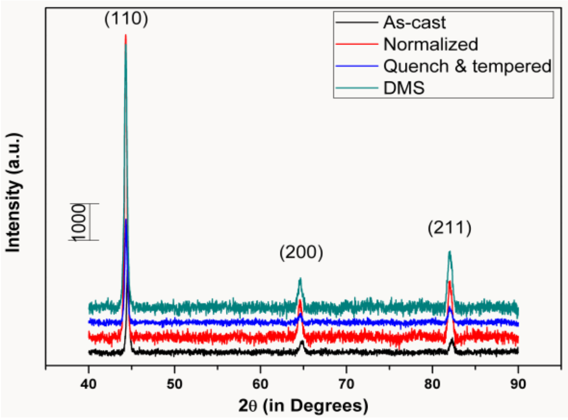

(a) XRD pattern for alloy SG-2

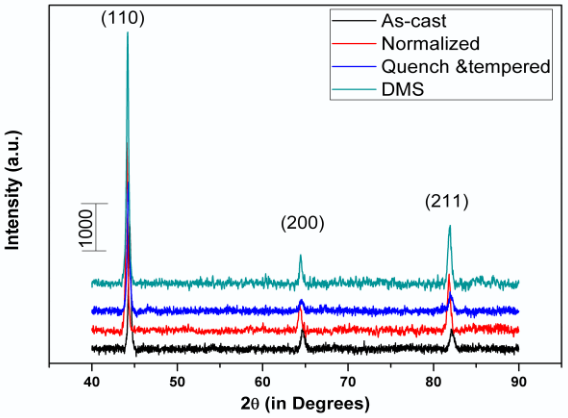

(b) XRD pattern for alloy SG-9

Fig. 1: XRD patterns for both alloys in as-cast and heat treated condition

3.2 *Metallographic characterization*

The microstructures of each heat treated & as-cast specimens are presented in Fig.2 & quantitative metallographic observations such as nodularity & volume fraction of different constituents are given in Table 3. It was observed that in as-cast condition for SG-9 alloy, [Fig.2 (a)] showed bull's eye ferritic/pearlitic matrix whereas in the case of alloy SG-2, [Fig.2 (b)] the matrix was fully ferritic. This is attributed to the presence of higher Silicon content which is an active promoter of ferrite & helps in dissolving the Carbon atoms into the matrix [11, 12,]. Dissolution of Carbon atom & other alloying elements present in lower quantity is evident from the quantitative metallographic analysis showing higher ferrite content (71%) & lower graphite content (29%) than SG-9. However, although there are elements like Copper & Molybdenum, which are present in very less quantity & promotes the formation of the pearlitic matrix, still not sufficient to overcome the effect of Si [13]. Normalized specimen of both the alloys showed pearlitic microstructure with some amount of ferrite, [Fig.2 (c) & (d)]. The high content of Si & Cr again overcome the combined effect of pearlite promoting elements like Molybdenum, Copper & higher Nickel content [14] & reduced the formation of pearlite, which is evident from the quantitative metallographic analysis showing 29% less pearlite in the SG-2 normalized specimen. Tempered martensitic microstructure [Fig.2 (e) & (f)] was obtained by reheating the specimens at 500°C for 120 minutes after quenching in mineral oil for both the alloys. However, a very small amount of proeutectoid ferrite was retained in SG-9 alloy [Fig.2 (e)]. It was quite interesting to note that, both the alloys when treated at an intercritical austenitizing temperature (800°C) produce a microstructure with stable martensite (M) and ferrite (F) [15], Fig.2 (g) & (h). From the quantitative analysis, it was observed that alloy SG-2 had higher ferrite volume fraction than alloy SG-9, whereas the latter had higher martensite volume fraction. In as-cast condition both the alloys were observed to have Type II (relatively spherical) graphite nodules with 96% and 94% nodularity for SG-9 & SG-2 respectively, however after heat treatment, it was found that both the alloys had Type I (completely spherical) graphite nodules. It was observed that there was a change in nodularity & volume fraction of different phases, caused by heat treatment processes for both SG-9 & SG-2. There was an increment of 1.28% nodularity & 79.26% in pearlite area fraction for normalized specimen & decrement of 6.54% in nodularity for quench & tempered specimen as compared to the as-cast specimen for alloy SG-9. On the other hand, for SG-2, the nodularity was observed to be increased by 1.64% & 5.16% in normalized and quench & tempered specimen respectively. The nodule count was observed to be highest for quench and tempered specimens and was lowest for the dual matrix structured specimens. It can be noticed that heat treated specimens have higher nodule count as compared to the as-cast specimen due to the rate of cooling which restricts the diffusion of carbon atoms into the matrix and enhances the graphite nucleation sites, except in the case of inter critically treated specimens.

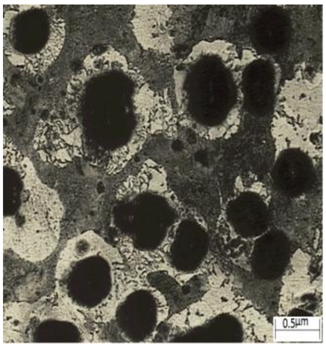

Fig. 2(a): SG-9 As-cast

Fig. 2(b): SG-2 As-cast

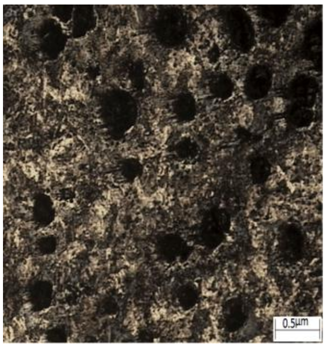

Fig. 2(c): SG-9 Normalized

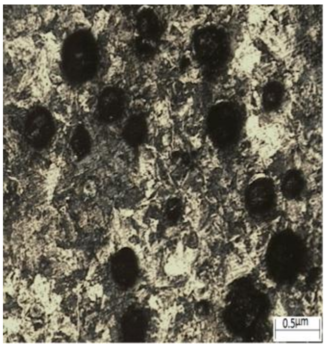

Fig. 2(d): SG-2 Normalized

Fig. 2(e): SG-9 Quench & tempered

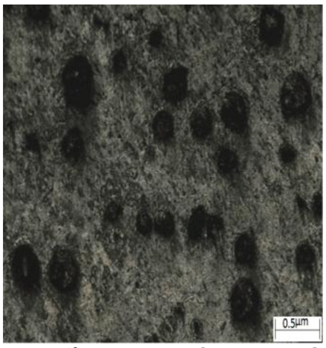

Fig. 2(f): SG-2 Quench & tempered

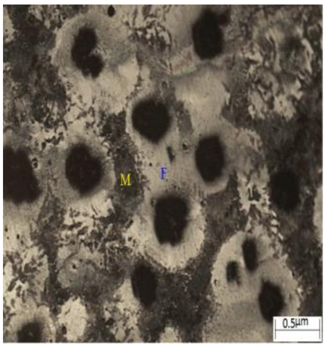

Fig. 2(g): SG-9 DMS

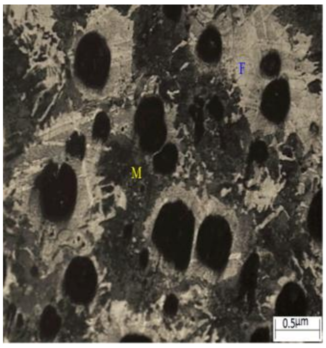

Fig. 2(h): SG-2 DMS

Fig. 2: Matrix microstructure of as-cast and heat treated specimens for alloys SG-2 and SG-9

Table 3: Quantitative metallographic observation of respective as-cast & heat treated specimens.

Specimen ID	Nodularity	Nodule Count (per mm^2)	Ferrite Area Fraction	Tempered Martensite Area Fraction	Martensite Area Fraction	Graphite Area Fraction	Pearlite Area Fraction
SG-2 As-Cast	94%	36	71%	----	----	29%	----
SG-2 Normalized	95%	40	21.5%	----	----	39%	46.5%
SG-2 Quench & Tempered	99%	43	----	79%	----	21%	----
SG-2 DMS	100%	25	38%	----	42%	20%	----
SG-9 As-Cast	96%	28	48%	----	----	38.5%	13.5%
SG-9 Normalized	97%	36	19.5%	----	----	15%	65.5%
SG-9 Quench & Tempered	89.5%	39	2.5%	57.5%	----	40%	----
SG-9 DMS	100%	18	32%	----	46%	22%	----

3.3 Mechanical properties

The strength, hardness, % elongation & impact energy values of respective as-cast & heat treated specimen are presented in Fig. 3. Highest strength values were obtained in the case of quench & tempered specimens along with Vickers hardness values for SG-9 & SG-2 alloys respectively. On the other hand lowest UTS & hardness for alloy SG-9 with ferritic/pearlitic matrix & that of alloy SG-2 with fully ferritic matrix were obtained. The high strength & hardness values obtained were due to the tempered martensitic matrix. Further the thermal stress developed during quenching was removed on reheating the specimens that yield in a fair amount of ductility for both the alloys [16, 17]. Ductility & Izod impact energy values for both alloys in as-cast condition were found to be maximum, fully ferritic matrix showed 32.22% ductility & impact energy of 28.29J whereas pearlitic/ferritic matrix showed 18.95% ductility & impact energy of 13.73J. Evidence of direct relationship of tensile strength with pearlite content [11] was found through quantitative metallographic analysis, which showed a higher pearlite content for SG-9 normalized specimen than SG-2 normalized. It is clear that the hard phases viz. pearlite & tempered martensite developed due to air cooling and oil quenching respectively are responsible for the increase in strength & reduction in ductility compared to the soft as-cast matrices. The quantitative metallographic analysis revealed that with increasing ferrite area fraction the % elongation & impact energy is increasing. From Table 3 it can be seen that there was a minor decrement in nodularity of SG-2 as-cast specimen but due to higher ferrite content as compared to SG-9 as-cast specimen, the ductility value of former is greater. On the other hand in case of normalized condition specimen with higher nodularity, SG-9 was more ductile, tougher and stronger than SG-2. However, the hardness value was higher in the later case. It can be noticed that after each treatment some amount of ferrite content was present in the event of alloy SG-2 due to higher amount of Si & Cr, resulting higher hardness value for each type of treatment as compared to SG-9 & can be attributed to the fact that addition of Mo & increased amount of Ni that strengthened the ferrite matrix via solid solution hardening [18].

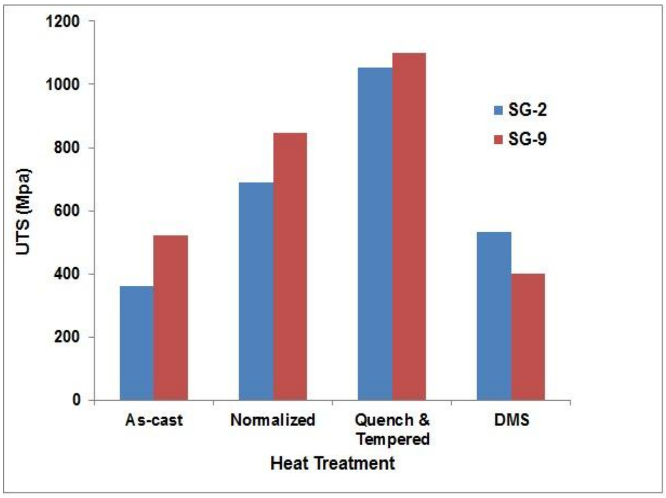

Fig. 3 (a): UTS of as-cast & heat treated specimens for both alloys.

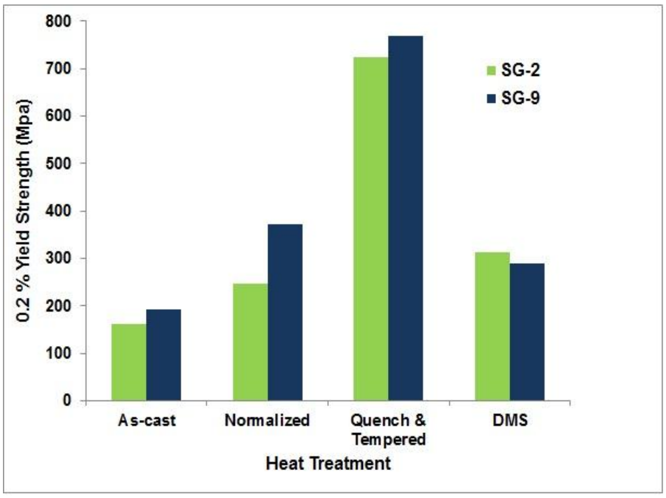

Fig. 3 (b): 0.2% Yield strength of as-cast and heat treated specimens for both alloys

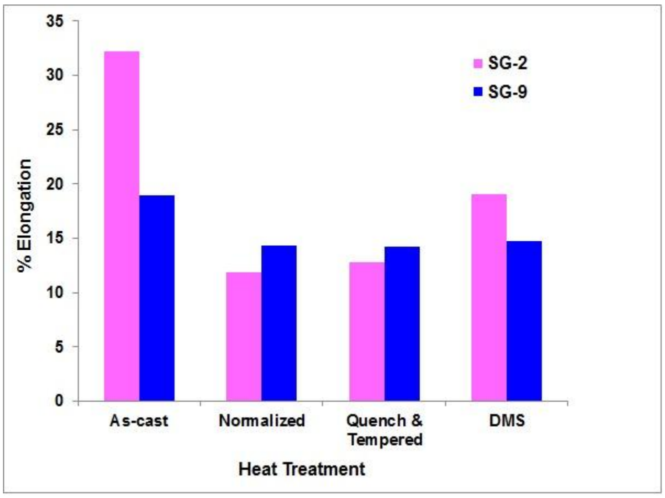

Fig. 3 (c): % Elongation of as-cast & heat treated specimen for both alloys

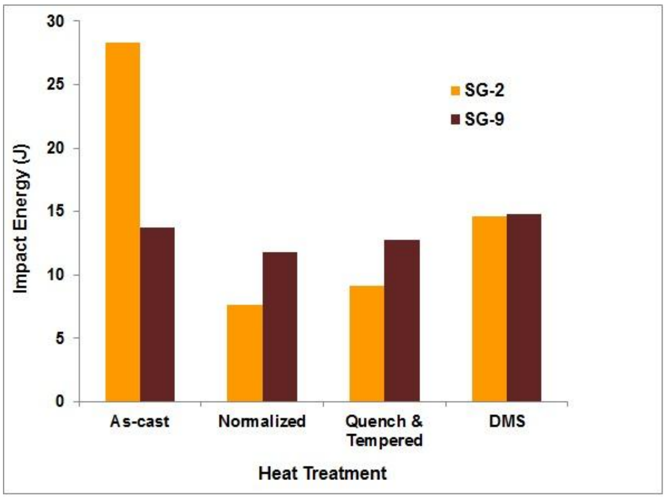

Fig. 3 (d): Izod impact energy of as-cast & heat treated specimens for both alloys

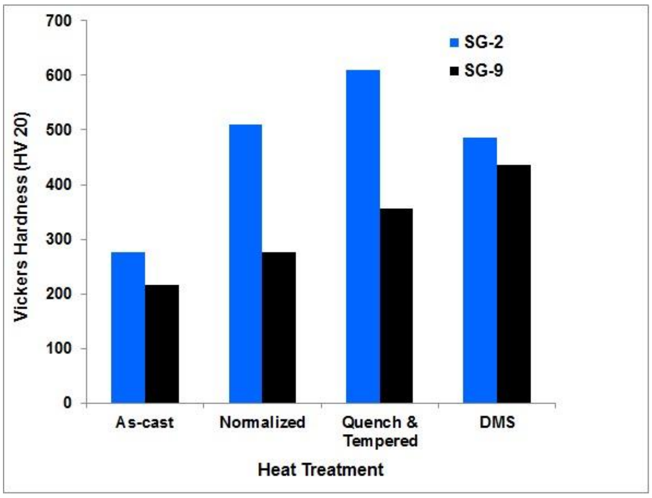

Fig. 3 (e): Hardness of as-cast & heat treated specimen for both alloys

3.4 Fractographic observation

Naked eye observation of fracture surfaces after tensile test indicated ductile mode failure by dull & irregular shape appearance for as-cast specimens & brittle failure mode by shiny & flat fracture surfaces appearance for normalized and quench & tempered specimens. The SEM observation of SG-9 as-cast specimens at 250X, [Fig. 4(a)] showed low energy stress paths/river markings characterizing the brittle mode of failure, but when the magnification was increased to 500X, [Fig. 4(b)] dimples were appeared around the graphite nodules as well as in the matrix indicating the ductile mode of failure. On the other hand, SG-2 as-cast specimen with fully ferritic matrix seemed to be failed in a ductile mode characterized by the dimples present around the graphite nodule & in the matrix [Fig. 4(c)]. Specimens with hard pearlitic matrix [Fig. 4(d) & Fig. 4(e)] observed to have low energy stress paths along with cleavage planes indicating the brittle mode of failure [14]. The quench & tempered specimens also had river marking & cleavage planes when observed at 250X [Fig. 4(f)] for alloy SG-9 indicating the brittle mode of failure, but at 500X, [Fig. 4(g)] shallow dimples were observed around the graphite nodules suggesting a mixed mode of failure [19, 20]. Similar kind of phenomenon was also observed for alloy SG-2 at quench & tempered heat treated condition, i.e., at magnification 250X, [Fig. 4(h)] low-intensity stress paths suggesting a brittle mode of failure & at 500X, [Fig. 4(i)] shallow dimples were present which confirms the mixed mode of failure. The dual matrix structured specimens were observed to have mixed mode of failure [Fig. 4(j) & (k)], due to the presence of both hard martensitic and soft ferritic matrix [21].

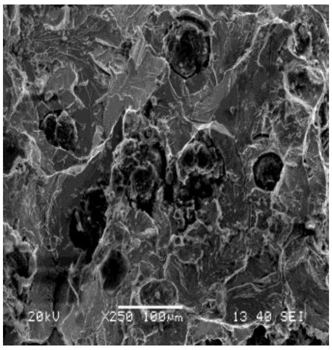

Fig. 4(a): SG-9 As-cast at 250X

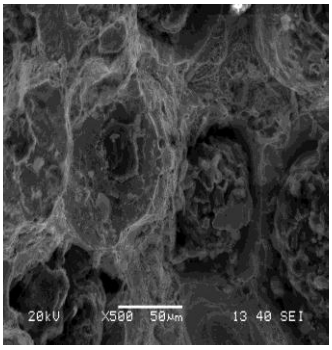

Fig. 4(b): SG-9 As-cast at 500X

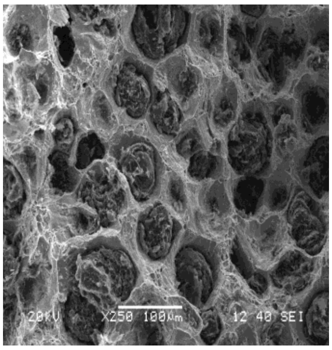

Fig. 4(c): SG-2 As-cast at 250X

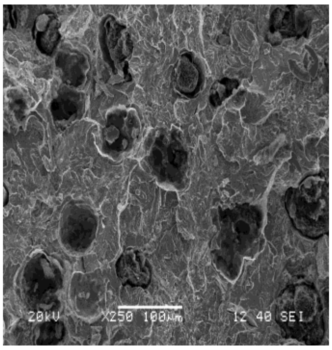

Fig. 4(d): SG-9 Normalized at 250X

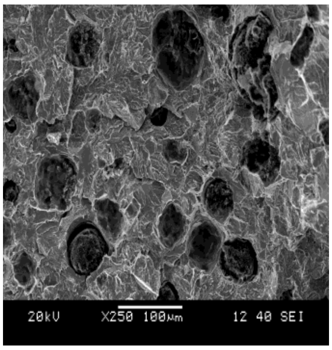

Fig. 4(e): SG-2 Normalized at 250X

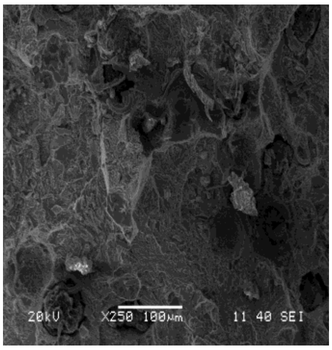

Fig. 4(f): SG-9 quench & tempered at 250X

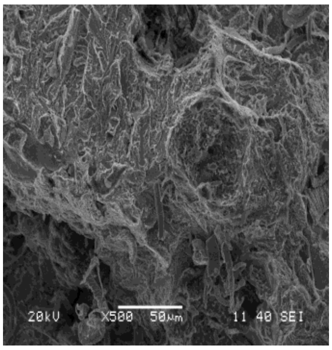

Fig. 4(g): SG-9 quench & tempered at 500X

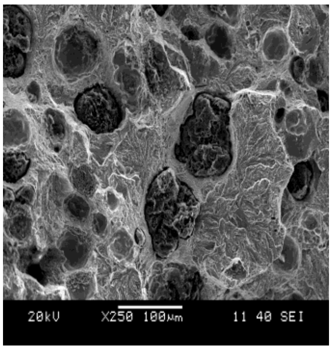

Fig. 4(h): SG-2 quench & tempered at 250X

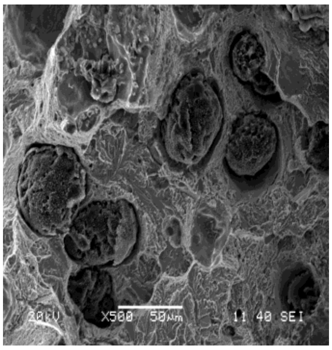

Fig. 4(i): SG-2 quench & tempered at 500X

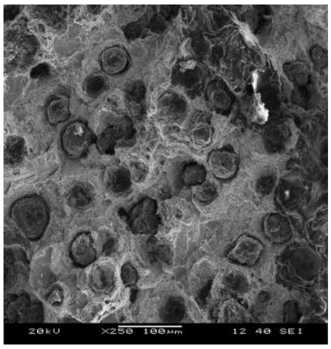

Fig. 4(j): SG-9 DMS at 250X

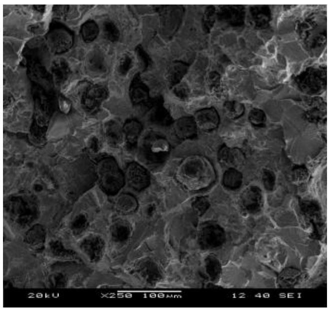

Fig. 4(k): SG-9 DMS at 250X

Fig.4: SEM micrographs of specimens fractured under uniaxial tensile loading.

IV. CONCLUSIONS

Ductile iron specimens with varying alloying element were subjected to normalizing & hardening & tempering heat treatment processes to investigate the microstructure-strength relationship. Experimental results reveal that both the ductile iron materials can be used for nuclear fuel transport cask fabrication. Following conclusions are drawn from the current study;

1. The as-cast ferritic & bull's eye ferritic/pearlitic structure were converted into pearlitic microstructure after normalizing heat treatment, which enhanced the strength & hardness of respective specimen at the expense of ductility & impact resistance.

2. Quench & tempered specimens have highest strength & hardness values with a fair amount of ductility due to the removal of thermal stress developed by reheating the specimens after quenching in oil & reducing stress concentration effect by breaking the martensite needles.

3. Ductile mode of failure was found to be dominant for the ferritic matrix, whereas the mixed mode of fracture was observed for ferritic/pearlitic matrix as well as tempered martensitic matrix. On the other hand, pearlitic matrix appeared to have brittle nature of fracture characterized river marking.

4. Alloying elements such as Si & Cr was found to have an effect on ferrite stabilizing characteristic even after normalizing & hardening & tempering heat treatment process, whereas Mo & Ni helped in improving hardness by strengthening ferrite via solid solution strengthening.

5. The mechanical properties along with morphological aspects obtained for both the alloys in as-cast as well as heat treated conditions specimens of are well within that recommended in ASTM A874 Draft Specification Material Properties, hence can be used for fabrication of nuclear fuel cask.

V. ACKNOWLEDGMENT

The authors deeply acknowledge the financial support provided by Board of Research in Nuclear Science, India to carry out this investigation. The authors also express their gratitude towards the help of L&T Kansbahal, India for providing test blocks for this investigation & M/S Steelage Engineering works, Rourkela, India for their immense help during machining of tensile and impact specimens.

VI. REFERENCES

[1] E.M.El-Banna, "A study of ferritic centrifugally cast ductile cast iron," Mater. Lett., vol. 20, pp. 99-106, April 1994.

[2] Yusuf Kayali, YılmazYalcin, SukruTaktak, "Adhesion and wear properties of boro-tempered ductile iron," Mater. Des., vol. 32, pp. 4295-4303, April 2011.

[3] M. A. Shaker, "A note on the effect of nodularization characteristics on the workability of quench hardened and tempered cast irons," J. Mater. Process. Technol., vol. 32, pp. 545-552, July 1991.

[4] R.C. Dommarco, M.E. Sousa, J.A. Sikora, "Abrasion resistance of high nodule count ductile iron with different matrix microstructures," Wear, vol. 257, pp. 1185-1192, October 2004.

[5] Jianghuai Yang, Susil K. Putatunda, "Effect of microstructure on abrasion wear behavior of austempered ductile cast iron (ADI) processed by a novel two-step austempering process," Mater. Sci. Eng., A, vol. 406, pp. 217-228, October 2005.

[6] Rong Zhou, Yehua Jiang, Dehong Lu, Rongfeng Zhou, Zhenhua Li, "Development and characterization of a wear resistant bainite/martensite ductile iron by combination of alloying and a controlled cooling heat-treatment," Wear, vol. 250, pp. 529-534, 2001.

[7] D.C. Wen and T.S. Lei, "Influence of Tempering on the Mechanical Properties of Austempered Ductile Iron," Mater. Trans., JIM, vol. 40, pp. 980-988, July 1999.

[8] Victor Kerlins. Modes of Fracture. In: Kathleen Mills, Joseph R. Davis, James D. Destefani, Deborah A. Dieterich, Heather J. Frissell, George M. Crankovic et.al. ASM Handbook, USA, ASM International, 1987, pp. 12-14.

[9] Ken B. Sorenson, Richard J. Salzbrenner, QUALITY ASSUARANCE ASPECTS IN USING DUCTILE CAST IRON FOR TRANSPORTATION CASKS, WMS papers, pp. 107-111, Phoenix, 1988.

[10] S. MOCHIZUKI and H. MATSUSHITA, "PHYSICAL PROPERTIES OF NODULAR CAST IRON FOR SHIPPING CONTAINERS AND SAFETY ANALYSIS BY FRACTURE MECHANICS," Nucl. Eng. Des., vol.94, pp. 309-316, 1986.

[11] R.A. Gonzaga, "Influence of ferrite and pearlite content on mechanical properties of ductile cast irons," Mater. Sci. Eng., vol. A567, pp. 1-8, January 2013.

[12] R. Aristizabal, R. Foley, A. Druschitz, "Intercritically AUSTEN ITIZED QUENC HED AN D TE MPERE D DUCT ILE IRON", Int. J. Metalcast., pp. 7-14, 2012.

[13] A.Alhussein, M.Risbet, A.Bastien, J.P.Chobaut, D.Balloy, J.Favergeon, "Influence of silicon and addition elements on the mechanical behavior of ferritic ductile cast iron," Mater. Sci. Eng., A, vol. 605, pp. 222–228, March 2014.

[14] Cheng-Hsun Hsu, Ming-Li Chen, Chia-Jung Hu, "Microstructure and mechanical properties of 4% cobalt and nickel alloyed ductile irons," Mater. Sci. Eng. A, vol. 444, pp. 339-346, 2007.

[15] S.C. Murcia, M.A.Paniagua, E.A.Ossa, "Development of as-cast dual matrix structure (DMS) ductile iron," Mater. Sci. Eng., A, vol.566, pp. 8-15, 2013.

[16] Y. Sahin, M. Erdogan. M. Cerah, "Effect of martensite volume fraction and tempering time on abrasive wear of ferritic ductile iron with dual matrix," Wear, vol. 256, pp. 196-202, January 2008.

[17] Ali M. Rashidi, M. Moshrefi-Torbati, Effect of tempering conditions on the mechanical properties of ductile cast iron with dual matrix structure(DMS), Mater. Lett., vol. 45, pp. 203-207, September 2000 .

[18] G.S.Cho, K.H.Choe, K.W.Lee and A.Ikenaga, "Effects of Alloying Elements on the Microstructures and Mechanical Properties of Heavy Section Ductile Cast Iron," J. Mater. Sci. Technol., vol. 23, pp. 97-101, May 2006.

[19] R.K.BEHERA, S.C.MISHRA, S.SEN, "Characterization of Heat Treated Ductile Iron Through Fractographic Analysis," Int. Conf. Emerging Materials and Processes, CSIR-IMMT Bhubaneswar, India, p.419, February 2014.

[20] R.K.BEHERA, B.P.MAHTO, J.S.DUBEY, S.C.MISHRA, S.SEN, "Property Enhancement of Cast Iron to be Used for Nuclear Cask," Int. J. Minerals, Met. Mater., unpublished.

[21] Yahya Hoque Mozumder, Ranjan Kumar Behera, Sudipta Sen, "Influence of intercritical austenitizing temperature and different quenching medium on mechanical properties and wear behaviour of dual matrix structured ductile iron," Orissa J. Phys., Vol. 22, pp. 39-51, February 2015.